Spectrochimica Acta Part A: Molecular and Biomolecular Spectroscopy 224 (2020) 117417

Contents lists available at ScienceDirect

Spectrochimica Acta Part A: Molecular and Biomolecular Spectroscopy

journal homepage: www.elsevier.com/locate/saa

Dual-aptamers labeled polydopamine-polyethyleneimine copolymer dots assisted engineering a fluorescence biosensor for sensitive detection of *Pseudomonas aeruginosa* in food samples

Zitao Zhong [1], Ran Gao [1], Qingmei Chen, Li Jia*

Ministry of Education Key Laboratory of Laser Life Science & Institute of Laser Life Science, College of Biophotonics, South China Normal University, Guangzhou 510631, China

ARTICLE INFO

Article history:
Received 6 May 2019
Received in revised form 12 July 2019
Accepted 22 July 2019
Available online 23 July 2019

Keywords:
Polydopamine-polyethyleneimine
Polymer dots
Aptamer
Bacteria
Fluorescence detection
Food samples

ABSTRACT

To ensure the food security and protect public health, development of rapid and reliable approaches to detecting foodborne pathogens is of great significance. In this study, polydopamine-polyethyleneimine (PDA-PEI) copolymer dots are prepared via the self-polymerization of dopamine and cross-linking with branched PEI at room temperature. The PDA-PEI copolymer dots are very stable against photobleaching, extreme pH, as well as high ionic strength. They are used as a fluorescent probe to fabricate a biosensor for rapid and sensitive detection and quantification of *Pseudomonas aeruginosa* (*P. aeruginosa*). In the biosensor, dual-aptamers of *P. aeruginosa* are used to label PDA-PEI copolymer dots. Compared to single aptamer labeled PDA-PEI dots, the dual-aptamers labeled PDA-PEI dots endow the biosensor with enhanced sensitivity for target pathogen. The fluorescence biosensor demonstrates a wide linear response to *P. aeruginosa* in the concentration range of 10^1–10^7 cfu mL^{-1} with acceptable selectivity. The limit of detection is calculated to be 1 cfu mL^{-1}. The whole detection process can be finished in 1.5 h. The feasibility of the fabricated biosensor is verified by successful determination of *P. aeruginosa* in skim milk, orange juice, and popsicle samples. The biosensor provides an alternative and attractive platform for rapid and sensitive detection of bacteria in food products.

1. Introduction

Food safety is the premise of healthy life. However, the widespread pathogenic bacteria in our daily life and natural environment pose a great worldwide threat to food safety and public health [1]. Thus, development of rapid and reliable approaches for pathogenic bacteria is imperative to increase protection level of public health and ensure the safety of consumers.

The traditional culture method as the “gold standard” usually takes several days to obtain reliable results. The lengthy waiting period associated with the method is discouraging. In order to timely detect pathogens contamination in food products and prevent the outbreak of foodborne illness caused by pathogens, various rapid detection approaches for pathogens have been developed and mainly include polymerase chain reaction (PCR)-based, immunology-based, as well as biosensor-based methods [2]. Among these methods, fluorescence biosensors are considered as an attractive technology for rapid detection of foodborne pathogens due to their excellent sensitivity and portability to be used on-site [3].

Fluorescent tags are an indispensable component for fabrication of fluorescence biosensors. Organic fluorescent dyes, such as carboxyfluorescein [4], fluorescein isothiocyanate [5], and acridine orange [6], have been utilized as fluorescent tags to engineer biosensors for pathogens detection. However, these traditional organic fluorescent dyes require distinctive excitation wavelengths and frequently produce overlapping emission peaks, thus leading to the difficulty in multiplex detection. Another major shortcoming is the susceptibility to photobleaching. In comparison with organic dyes, fluorescent nanomaterials demonstrate superior properties, such as broad absorption spectrum, narrow and size-tunable emission spectrum, and good stability against photobleaching [7–9]. Benefiting from their intriguing properties, some fluorescent nanomaterials, such as semiconductor quantum dots [10], carbon dots [11], graphene quantum dots [12], upconversion nanoparticles [13], and metal organic frameworks [14], have been used as the building blocks to fabricate biosensors for detection of pathogens. Compared to these fluorescent nanomaterials, polymer-based fluorescent nanomaterials exhibit desirable biocompatibility and biodegradability [8]. Especially, preparation of the fluorescent nanoparticles via the self-polymerization of dopamine (DA) is facile and these polydopamine (PDA) based-nanomaterials have been successfully applied for biological imaging applications [15–17].

* Corresponding author.
E-mail address: jiali@scnu.edu.cn (L. Jia).
[1] The first two authors contributed equally to this work.

https://doi.org/10.1016/j.saa.2019.117417
1386-1425/

Inspired by the remarkable features of PDA-based fluorescent nanoparticles, we tried to investigate their possibility in fabrication of fluorescence biosensor for detection of pathogens.

In order to ensure the selectivity of a fabricated fluorescence biosensor, the target-recognition element is another indispensable component. Nucleic acid aptamers as the recognition elements exhibit superior characteristics including good affinity and specificity, high resistance against denaturation, convenient generation, low cost, as well as easy and controllable modification [18]. They have been in conjugation with fluorescent tags to construct fluorescence biosensors for detection of various foodborne pathogens [19]. In most of biosensors, only one aptamer is used to recognize the target pathogen. Unlike small molecules and protein macromolecules, pathogens are micron-sized particles. Different components exist on the bacteria cell surface such as proteins, polysaccharides, and endotoxins. Thus, one aptamer is not enough to ensure the selectivity of fabricated biosensors for target pathogens.

In this study, the fluorescent PDA-polyethyleneimine (PDA-PEI) copolymer dots with green emission are synthesized at room temperature and in aqueous solutions using a facile one-pot method. They are very stable against photobleaching, extreme pH, as well as high ionic strength. More importantly, they contain a wealth of amino moieties, which endow them with good aqueous dispersibility and ease of modification. Inspired by the distinctive characteristics of PDA-PEI dots, we try to use them as a fluorescent tag to fabricate a biosensor for pathogens detection. They were separately labeled with two aptamers of *Pseudomonas aeruginosa* (*P. aeruginosa*). The dual-aptamers labeled PDA-PEI copolymer dots were combined for fluorescence detection of *P. aeruginosa* via simple centrifugation procedure. The high affinity and specificity of the dual-aptamers recognition system ensure the sensitivity and selectivity of the PDA-PEI dots-based biosensor. The feasibility of the fabricated biosensor was verified by successful determination of *P. aeruginosa* in skim milk, orange juice, and popsicle samples.

2. Experimental

2.1. Reagents and apparatus

All reagents were of analytical grade or better. Dopamine hydrochloride (DA·HCl) was acquired from Alfa Aesar (Shanghai, China). Branched PEI (Mw = 600) was purchased from Aladdin Co., Ltd. (Shanghai, China). Tris (hydroxymethyl) amino methane (Tris) and sodium chloride (NaCl) were purchased from Guangzhou Chemical Reagent Factory (Guangzhou, China). Sodium hydrate (NaOH) was supplied by Tianjin Damao Chemical Reagent Factory (Tianjin, China). 1-Ethyl-3-(3-dimethylaminopropyl) carbodiimide (EDC) and *N*-hydroxysuccinimide (NHS) were purchased from J&K Scientific Ltd. (Beijing, China). Hydrochloric acid (HCl) was obtained from Tianjin Fuyu Chemical Company (Tianjin, China). The aptamers were synthesized by Shanghai Sangon Biological Science & Technology Company (Shanghai, China). The sequences of aptamers are listed as follows: The carboxyl-modified *P. aeruginosa* aptamer$_1$: 5′-COOH-CCC CCG TTG CTT TCG CTT TTC CTT TCG CTT TTG TTC GTT TCG TCC CTG CTT CCT TTC TTG-3′ [20], aptamer$_2$: 5′-COOH-ATG CAC TCT TCT ATC GGT AGT TGA GGG TGC GG-3′ [21]. The aptamers were dissolved with deionized water and stored at −20 °C when not in use. Water used in the experiments was obtained from an ELGA water purification system (ELGA, London, UK).

Transmission electron microscopy (TEM) image was performed on a JEM-1400PLUS transmission electron microscope (JEOL, Tokyo, Japan). Ultraviolet-visible (UV—vis) spectra were determined on a K5600 microspectrophotometer (Beijing Kaiao Technology Development Company, Beijing, China). A Zetasizer NanoZS (Malvern, Worcestershire, UK) was applied to measure the zeta potentials and hydrodynamic size distribution. Fluorescence spectra were determined on a F-380A fluorescence spectrophotometer (Tianjin Gangdong Sci. & Tech. Development Co., Ltd., Tianjin, China). X-ray photoelectron spectroscopy (XPS) was measured on Thermo Escalab 250Xi (Thermo Fisher Scientific, Massachusetts, USA) with an Al (Kα = 1486.7 eV) X-ray source. ^{1}H and ^{13}C NMR spectra were recorded on a Bruker Avance NEO 600 (600 MHz) nuclear magnetic resonance (NMR) instrument using CD_3OD (water residue at 4.79 ppm as reference) as solvent.

2.2. Synthesis of PDA-PEI copolymer dots

The PDA-PEI copolymer dots were synthesized according to our previous work [22]. Briefly, 10 mg DA·HCl and 10 mg branched PEI were dissolved in 10 mL Tris-HCl solution (10 mM, pH 8.5). Subsequently, the mixture was stirred for 12 h at 500 rpm under ambient temperature in the dark. Afterwards, the solution was filtered through a 0.22 μm membrane, then dialyzed against deionized water through a 1000 MWCO dialysis membrane. Finally, the as-prepared PDA-PEI copolymer dots were stored at 4 °C for further use.

2.3. Preparation of aptamers modified PDA-PEI copolymer dots

In brief, freshly prepared EDC solution (100 μL, 10 mM) and NHS solution (100 μL, 10 mM) were successively added to an Eppendorf tube containing 65 μL COOH-aptamer$_1$ (10 μM) for activating carboxyl groups. The mixture was reacted at 37 °C with shaking for 30 min. Next, 120 μL PDA-PEI copolymer dots solution (4.5 mg mL^{-1}) was added to the mixture and reacted for 30 min at 37 °C in the dark. The aptamer$_1$ modified PDA-PEI dots (aptamer$_1$@PDA-PEI) were prepared. The aptamer$_2$@PDA-PEI dots were prepared by the same procedure. Then aptamer$_1$@PDA-PEI and aptamer$_2$@PDA-PEI solutions were mixed and dialyzed against deionized water through a 3500 MWCO dialysis membrane to remove free aptamers and PDA-PEI copolymer dots. Finally, the aptamers@PDA-PEI copolymer dots inside the dialysis bag were collected and stored at 4 °C for further use.

2.4. Bacterial strain culturing

The bacterial strain *P. aeruginosa* (ATCC15442) was grown in sterile Luria-Bertani (LB) media (10 mg mL^{-1} tryptone, 5 mg mL^{-1} yeast extract, 10 mg mL^{-1} NaCl, pH 7.4) at 37 °C overnight in a ZHWY-103B shaker (Shanghai Zhicheng Analytical Instrument Co., Ltd., Shanghai, China). The bacterial cells were collected by centrifugation at 10000 rpm (~ 9167 ×*g*) for 1 min and washed twice with Tris-HCl solution (20 mM, pH 7.4), and resuspended in Tris-HCl solution. The bacteria concentration was adjusted to the desired level by measuring the optical density (OD) at 600 nm (OD_{600}) (optical path length 10 mm). By plating the bacteria on LB plates, the amounts of bacteria per milliliter can be acquired by counting colony forming units (cfu) after incubation overnight at 37 °C. Bacterial culturing and sample handling were performed in a sterile clean room. All the containers were sterilized in an autoclave at 121 °C for 30 min before and after use.

2.5. Fluorescence detection of P. aeruginosa

After preparation of a desired concentration of *P. aeruginosa* (10^8 cfu mL^{-1}), a serial 10-fold dilution of samples were prepared from 10^1 to 10^7 concentrations using sterile Tris-HCl solution (20 mM, pH 7.4). The procedure for detection of *P. aeruginosa* is displayed in Fig. 1. Typically, 70 μL aptamers@PDA-PEI copolymer dots solution was respectively added to the tubes containing different concentrations of *P. aeruginosa* suspension (250 μL). Then the mixtures were incubated at 37 °C for 1 h. In this step, aptamers@PDA-PEI copolymer dots were used as fluorescent probes to capture target bacterial cells through the specific recognition of

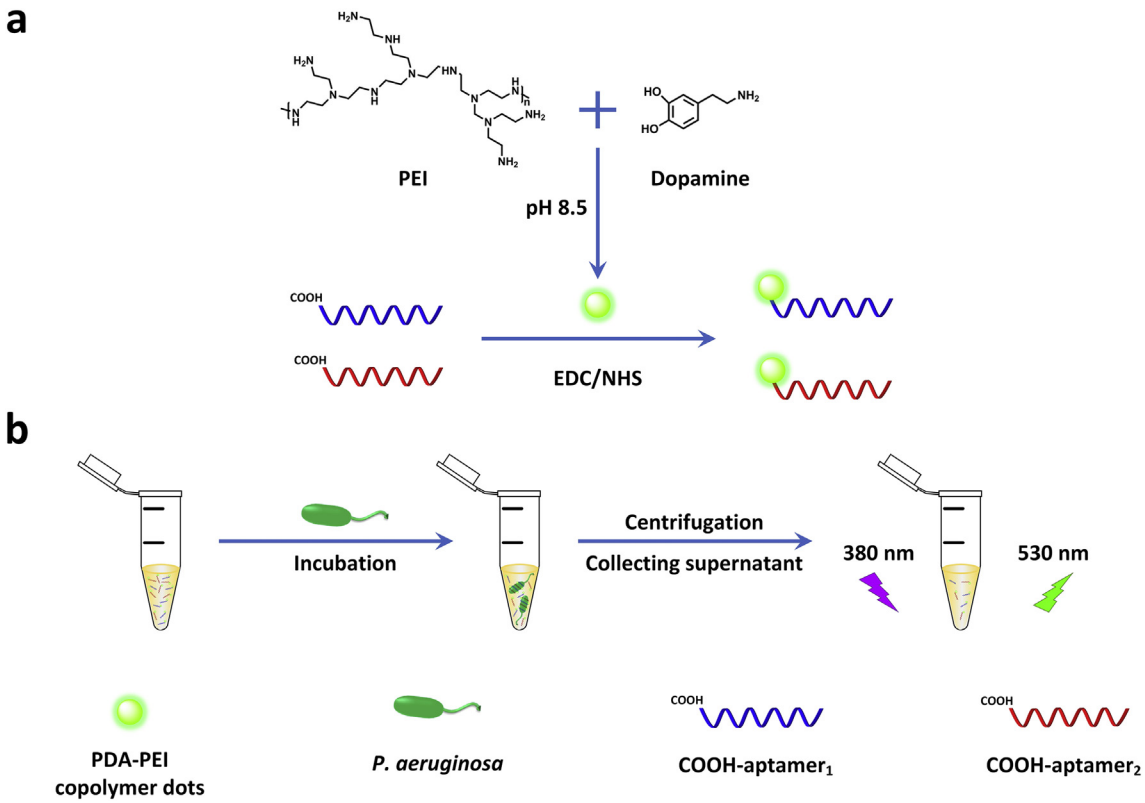

Fig. 1. Schematic illustration of the fabrication of dual-aptamers@PDA-PEI probe (a), and procedure for *P. aeruginosa* detection (b).

aptamers for *P. aeruginosa*. Subsequently, these mixtures were centrifuged at 8000 rpm (~ 5167 ×*g*) for 3 min to isolate the conjugate of *P. aeruginosa* and aptamers@PDA-PEI copolymer dots. After that, the supernatants were used for fluorescence detection. The fluorescence intensities were measured under the excitation/emission wavelengths of 380/530 nm by keeping the photomultiplier tube voltage at 700 V. The slit widths of both excitation and emission were 5.0 nm.

2.6. Application in real samples

Skim milk, orange juice, and popsicle samples were purchased from a local market. The skim milk and orange juice samples were diluted 100-fold using deionized water before determination. Popsicle samples were first to be melted, then diluted 100-fold using deionized water since the melted popsicle samples were viscous. The spiked samples containing different concentrations of *P. aeruginosa* were determined using the method described in previous section.

3. Results and discussion

3.1. Characterization

The structure information of PDA-PEI copolymer dots was characterized using NMR spectroscopy. The equivalent mass of PEI and DA was mixed for 6 h in the NMR tube. Then the mixture was directly analyzed by ^{1}H and ^{13}C NMR. Compared to the ^{1}H NMR spectra of DA and PEI (Fig. S1a), an additional peak at 8.11 ppm is observed in the ^{1}H NMR spectrum of PDA-PEI. This peak is assigned to the H protons of 5,6-dihydroxyindole, suggesting the presence of indole groups [23]. As shown in the ^{13}C NMR spectra (Fig. S1b), additional peaks between 110 and 120 ppm are observed in the ^{13}C NMR spectrum of PDA-PEI. These new peaks may be attributed to the C=C bonds of the indole groups in PDA-PEI [23]. The results confirm that PEI is incorporated into PDA-PEI copolymer dots.

The chemical composition of PDA-PEI copolymer dots was characterized by XPS. As shown in the full XPS spectra of PDA-PEI and DA (Fig. S2), the binding energy peaks of C (285.2 eV), N (405.6 eV), and O (536.6 eV) are observed. In comparison with DA (Fig. S2b), the peak of N element in PDA-PEI (Fig. S2a) was significantly enhanced. Atomic analysis displays that the percentages of N (N 1 s) in PDA-PEI dots and DA samples are 13.9% and 8.4%, respectively. The significant increase of the percentage of N element in PDA-PEI dots further suggests that PEI is successfully incorporated into PDA-PEI copolymer dots [16].

The particle size and morphology information of PDA-PEI copolymer dots were observed using TEM. As shown in the TEM image (Fig. 2a), the synthesized PDA-PEI copolymer dots have an average size of 4.7 ± 1.1 nm in diameter with good dispersity. The average hydrodynamic diameter of PDA-PEI copolymer dots in water was determined to be 125.6 ± 46.9 nm using dynamic laser scattering (DLS) (Fig. S3), which is larger than that obtained by TEM due to the hydration of abundant hydroxyl and amino groups, as well as the likely aggregation.

The UV–vis absorption spectrum of PDA-PEI copolymer dots in aqueous solution is shown in Fig. 2b. Two broad absorption peaks at 287 and 360 nm are observed. The appearance of the absorption peak at 287 nm is attributed to the DA oxidative products such as 5,6-dihydroxyindole as well as its oligomers [24,25]. The formation of Michael's-type adducts between different quinones and amines has been reported to result in an absorption peak between 340 and 400 nm [26]. Therefore, the absorbance peak at 360 nm suggests that PDA likely forms a Michael's-type adduct with PEI.

The photoluminescence properties of PDA-PEI copolymer dots were characterized by fluorescence spectroscopy. As shown in Fig. 2c, the maximum excitation intensity of PDA-PEI copolymer dots locates at 380 nm, and the maximum fluorescence intensity at 530 nm can be obtained using a 380 nm excitation wavelength. The quantum yield of PDA-PEI copolymer dots is measured to be 12.5% with respect to quinine sulphate (literature $\varphi = 55\%$ at 313 nm) in 0.1 M H_2SO_4

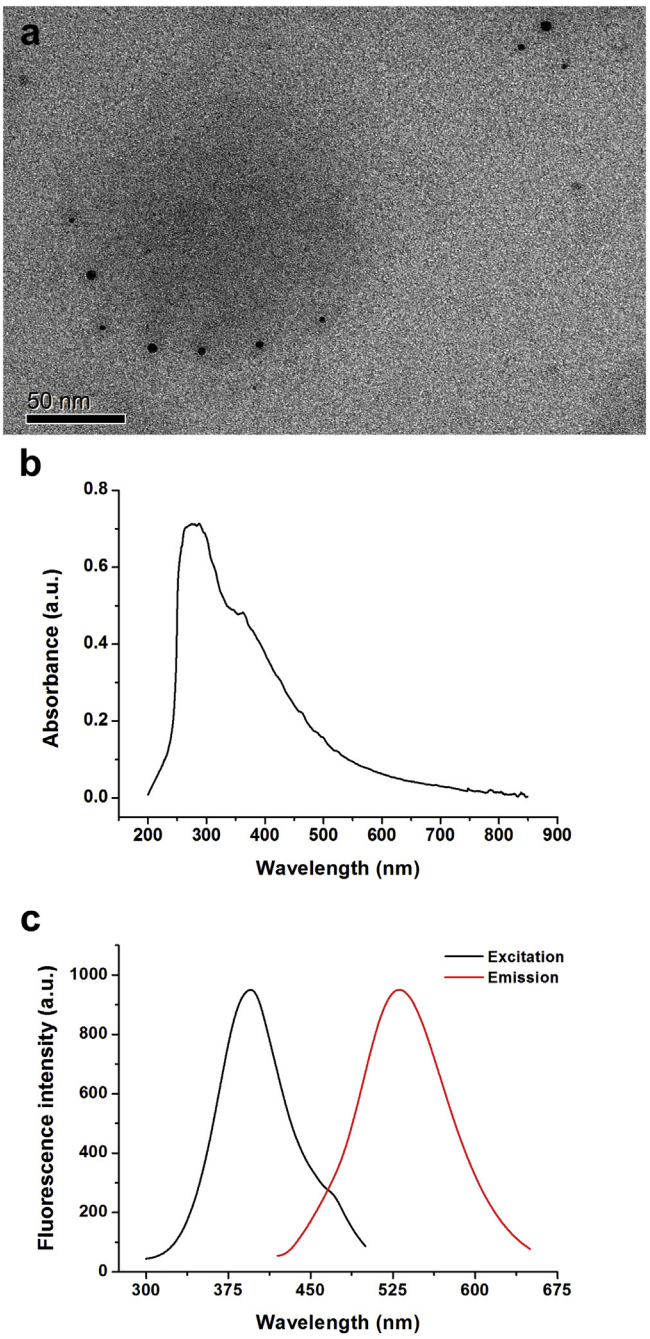

Fig. 2. TEM image (a), UV–vis absorption spectrum (b), excitation and emission spectra (c) of PDA-PEI copolymer dots.

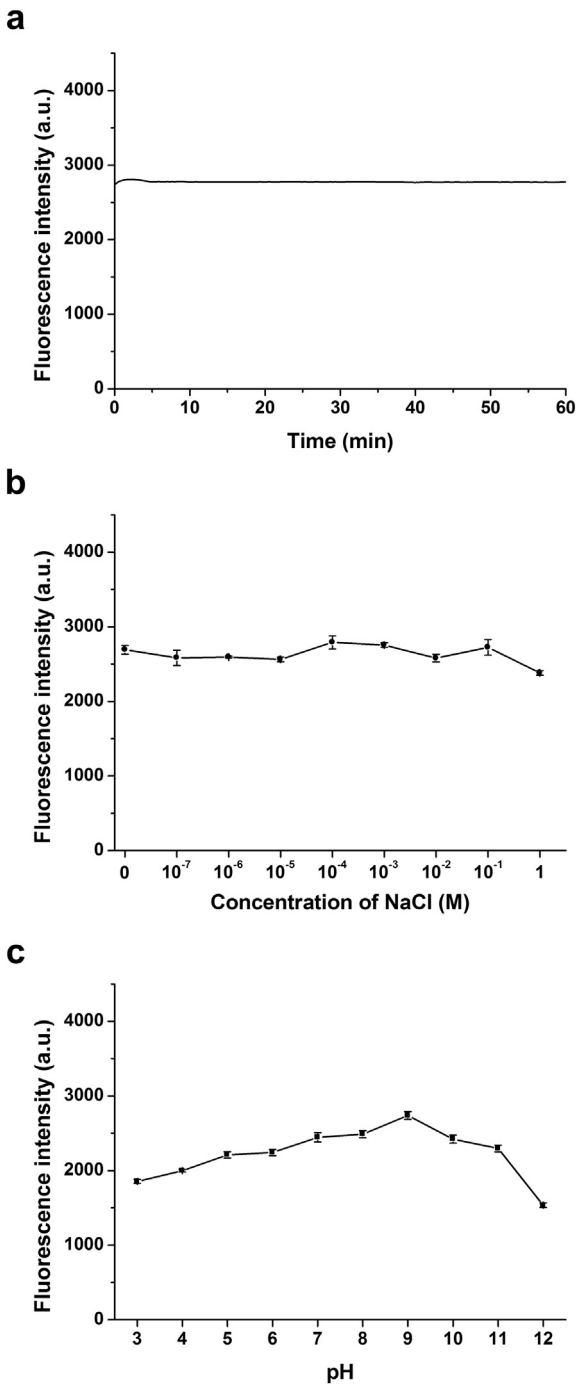

Fig. 3. Fluorescence intensity of PDA-PEI copolymer dots as a function of time under the illumination at 380 nm (a). Fluorescence intensities of PDA-PEI copolymer dots in 20 mM pH 7.4 Tris-HCl solutions containing different concentrations of NaCl (b). Fluorescence intensities of PDA-PEI copolymer dots at different pH values (c). The fluorescence intensities were measured under the excitation/emission wavelengths of 380/530 nm.

($n = 1.33$). Also, PDA-PEI copolymer dots demonstrate good stability against photobleaching, extreme pH, as well as high ionic strength (Fig. 3a, b, c). Fig. 3c shows that the fluorescence intensity of PDA-PEI copolymer dots exhibits little change in the pH range of 5–11, outside of which, the fluorescence intensity still remains >67%, compared to that at pH 9.0. The results suggest that the copolymer dots are suitable for the applications even under extreme pH conditions.

The photoluminescence properties of PDA-PEI dots in solvents with different ratios of tetrahydrofuran (THF) to water were also studied using fluorescence spectroscopy. As shown in Fig. S4, when the water fraction is larger than 40%, the fluorescence intensities of PDA-PEI dots under the excitation/emission wavelengths of 380/530 nm gradually decreases with the decrease of water fraction. The fluorescence emission peaks have a slight blue-shift. Further decreasing the water fraction in the range of 30–10%, the fluorescence intensities at 530 nm continuously decrease and a new peak located at around 435 nm appears. The abundant amino groups in PDA-PEI copolymer dots endow the dots with excellent aqueous dispersibility. The addition of THF might affect their dispersibility. DLS measurements were used to study the aggregation behavior of PDA-PEI copolymer dots. As evidenced by Fig. S5, the size of aggregates of PDA-PEI copolymer dots slowly increases with the decrease of water fraction in the range of 50–100%. Beyond 50%, the size of aggregates of PDA-PEI copolymer dots has a tremendous increase.

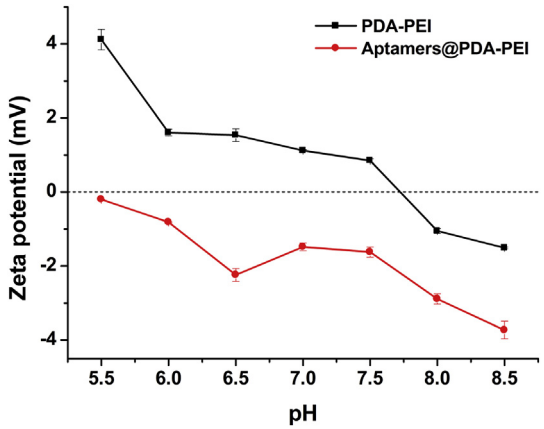

Fig. 4. Zeta potentials of PDA-PEI copolymer dots and dual-aptamers@PDA-PEI at different pHs.

The results demonstrate that the aggregation of PDA-PEI copolymer dots in the solvents containing THF causes the decreased fluorescence intensity at 530 nm and the blue-shift of the emission peak. In comparison with the fluorescence nanoparticles with aggregation-induced emission feature [9,27–29], PDA-PEI copolymer dots possess higher fluorescence quantum yield in aqueous solutions.

In order to demonstrate that aptamers were modified on the surface of PDA-PEI copolymer dots, the zeta potentials of PDA-PEI copolymer dots and aptamers@PDA-PEI dots were measured in 20 mM Tris-HCl solutions with different pH values ranging from 5.5 to 8.5. As shown in Fig. 4, there exists an inflection point (pH 7.7) for PDA-PEI copolymer dots. The zeta potentials of PDA-PEI copolymer dots are positive below pH 7.7, indicating that PDA-PEI copolymer dots take positive charges due to the protonation of amino groups in PDA and PEI. Above pH 7.7, PDA-PEI copolymer dots are negatively charged due to the ionization of phenolic hydroxyl groups in PDA. In the pH range of 5.5 to 8.5, aptamers@PDA-PEI dots are negatively charged. The difference in the zeta potential of PDA-PEI dots and aptamers@PDA-PEI-aptamers dots at the same pH demonstrates that the aptamers are successfully modified on the surface of PDA-PEI copolymer dots.

3.2. Designing fluorescence method for detection of *P. aeruginosa*

Initially, aptamer$_1$@PDA-PEI dots were used as a fluorescent probe to detect *P. aeruginosa*. In the detection procedure, aptamer$_1$ serves as a biorecognition element to selectively bind to the bacteria, and PDA-PEI copolymer dots as a signal reporter to quantify

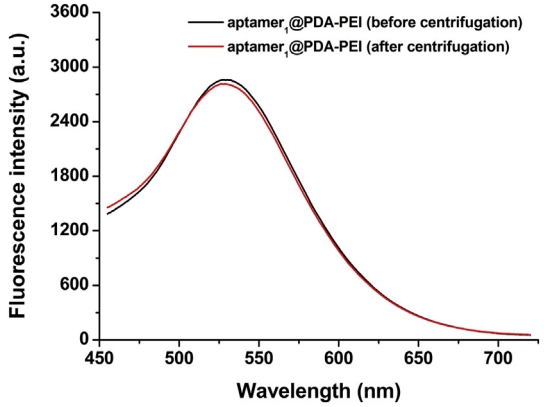

Fig. 5. Fluorescence emission spectra of the aptamer$_1$@PDA-PEI copolymer dots solution before and after centrifugation. The fluorescence intensities were measured under the excitation/emission wavelengths of 380/530 nm.

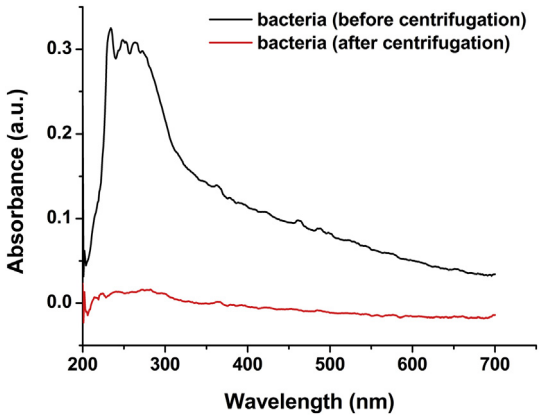

Fig. 6. UV–vis spectra of bacteria (10^7 cfu mL^{-1}) suspension before and after centrifugation.

the bacteria. In the presence of *P. aeruginosa*, the aptamer$_1$@PDA-PEI dots can specifically bind to the bacteria. Through the centrifugation at 8000 rpm for 3 min, the conjugate of bacteria and aptamer$_1$@PDA-PEI dots was isolated from the solution. The unbound aptamer$_1$@PDA-PEI dots remained in the supernatant. Thus, the amount of bacteria can be quantified through determination of the fluorescence intensity of the supernatant.

In order to prove the effectiveness of the method for detection of bacteria, two speculations need to be validated through experiments. The first one is that centrifugation at 8000 rpm for 3 min does not bring about the isolation of aptamer$_1$@PDA-PEI dots, but is enough to isolate bacteria from solution. The fluorescence intensity of aptamer$_1$@PDA-PEI dots solution before centrifugation under the excitation/emission wavelengths of 380/530 nm is about the same as that of supernatant after centrifugation of aptamer$_1$@PDA-PEI dots (Fig. 5). Compared to the absorbance of bacteria suspension (10^7 cfu mL^{-1}) at 250 nm, the obvious decrease in the absorbance of supernatant after centrifugation indicates that bacteria can be completely isolated from solution through centrifugation at 8000 rpm for 3 min (Fig. 6).

The second speculation is that PDA-PEI dots do not bind to the target bacteria. The PDA-PEI dots solution was first mixed with *P. aeruginosa*. Then the mixture was incubated at 37 °C for 30 min under shaking at 200 rpm in the dark. Subsequently, the mixture was centrifuged at 8000 rpm for 3 min to isolate the bacteria. As shown in Fig. 7, the fluorescence intensity of supernatant is about the same as that of PDA-PEI dots solution under the excitation/

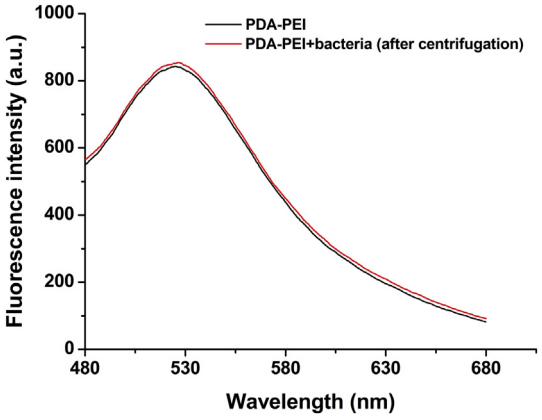

Fig. 7. Fluorescence emission spectra of the PDA-PEI copolymer dots and supernatant after centrifugation of mixture of PDA-PEI copolymer dots and bacteria (10^7 cfu mL^{-1}). The fluorescence intensities were measured under the excitation/emission wavelengths of 380/530 nm.

emission wavelengths of 380/530 nm. The result indicates that the bacteria do not bind to PDA-PEI dots.

The validation of the two speculations demonstrates that the aptamer$_1$@PDA-PEI dots-based fluorescence method can be applied for detection of *P. aeruginosa*. As shown in Fig. 8a, in the presence of target bacteria, the fluorescence intensity of supernatant decreases as expected. However, the decrease of the fluorescence intensity of supernatant along with the increase of bacteria concentration does not demonstrate significant difference, which is not suitable for accurate quantification. Since bacteria are microsized particles and different components exist on the bacteria cell surface, different aptamers have different binding sites on the surface of bacteria cell. Thus, aptamer$_2$@PDA-PEI dots were applied for detection of *P. aeruginosa*. Fig. 8b demonstrates a similar result to that obtained by using aptamer$_1$@PDA-PEI dots. These results bring up a hint that the combination of aptamer$_1$@PDA-PEI dots and aptamer$_2$@PDA-PEI dots could enhance the sensing performance for detection of target bacteria because dual aptamers can simultaneously bind to different moieties on cell surface. Excitingly, the expected result is obtained, as shown in Fig. 8c. The dual-aptamers@PDA-PEI dots significantly enhance the sensitivity for target bacteria. This result suggests that the usage of multiple aptamers labeled dots can improve the detection sensitivity more effectively than by single aptamer labeled dots for target bacteria detection.

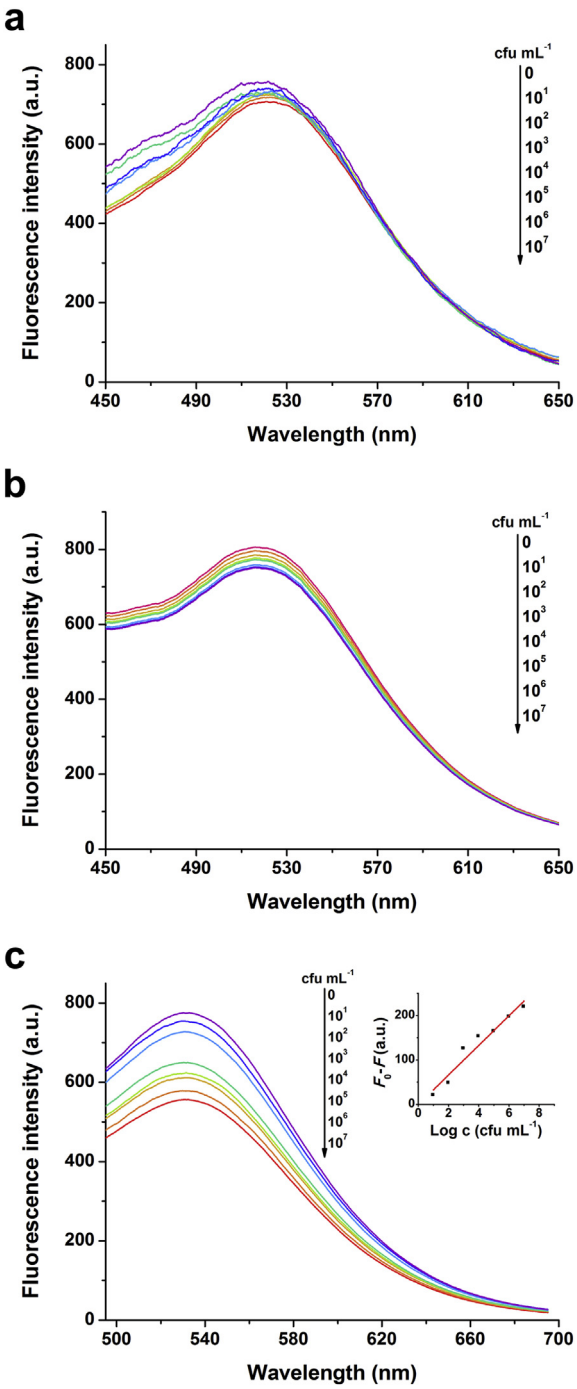

Fig. 8. (a) Fluorescence spectra of supernatant after centrifugation of mixture of aptamer$_1$@PDA-PEI and different concentrations of *P. aeruginosa*. (b) Fluorescence spectra of supernatant after centrifugation of mixture of aptamer$_2$@PDA-PEI and different concentrations of *P. aeruginosa*. (c) Fluorescence spectra of supernatant after centrifugation of mixture of dual-aptamers@PDA-PEI and different concentrations of *P. aeruginosa*. The inset shows the linearity of the decrease in fluorescence intensity against the logarithm of concentration of *P. aeruginosa* (cfu mL^{-1}). The fluorescence intensities were measured under the excitation/emission wavelengths of 380/530 nm.

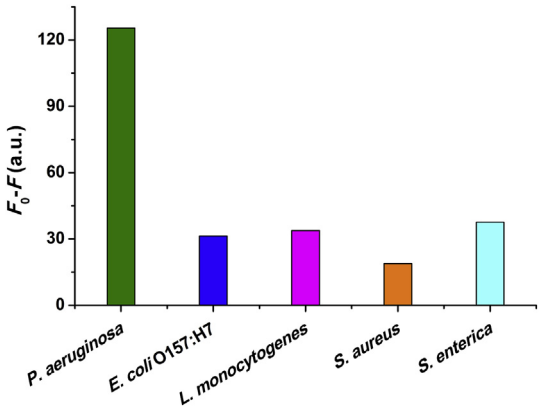

Fig. 9. Specificity investigation of the method towards *P. aeruginosa* and different controls ($n = 3$). The concentration of each bacterium was 10^3 cfu mL^{-1}. Experimental conditions: bacteria suspension in 250 μL Tris-HCl (20 mM, pH 7.4); aptamers@PDA-PEI in 70 μL Tris-HCl (20 mM, pH 7.4); incubation temperature, 37 °C; incubation time, 1 h. The fluorescence intensities were measured under the excitation/emission wavelengths of 380/530 nm.

3.3. Analytical performance

Quantitative analysis was achieved by measuring the fluorescence intensity of the unbound aptamers@PDA-PEI in the supernatant (λex/em = 380/530 nm). As shown in Fig. 8c, the decrease of fluorescence intensity is directly proportional to the logarithm of *P. aeruginosa* concentration in the range from 10^1 cfu mL^{-1} to 10^7 cfu mL^{-1}. The calibration plot (inset of Fig. 8c) fits a regression equation of $F_0 - F = 33.26 \log c - 0.3214$ with a determination coefficient of $R^2 = 0.9363$, where F_0 and F are the fluorescence intensities of PDA-PEI-aptamers in the absence and presence of *P. aeruginosa*, and c represents the concentration of *P. aeruginosa* (cfu mL^{-1}). The limit of the detection (LOD) is calculated to be 1 cfu mL^{-1} (LOD = 3SD/slope, $n = 10$).

Table 1
Recovery experiments of *P. aeruginosa* in real samples using the aptamers@PDA-PEI dots-based biosensor ($n = 6$).

Sample	Spiked (cfu mL^{-1})	Found (cfu mL^{-1})	Recovery (%)	RSD (%)
Milk 1	$(4.14 \pm 0.36) \times 10^2$	$(3.81 \pm 0.17) \times 10^2$	92.0	4.5
Milk 2	$(1.35 \pm 0.13) \times 10^3$	$(1.30 \pm 0.07) \times 10^3$	96.3	5.4
Juice 1	$(8.12 \pm 0.71) \times 10^2$	$(8.73 \pm 0.23) \times 10^2$	108	2.6
Juice 2	$(1.86 \pm 0.12) \times 10^3$	$(1.70 \pm 0.11) \times 10^3$	91.4	6.5
Popsicle 1	$(6.13 \pm 0.22) \times 10^2$	$(6.18 \pm 0.24) \times 10^2$	101	3.9
Popsicle 2	$(3.61 \pm 0.31) \times 10^3$	$(3.69 \pm 0.19) \times 10^3$	102	5.1

Table 2
Comparison of the aptamers@PDA-PEI-based biosensor with previously reported fluorescent methods targeting at detection of *P. aeruginosa*.

Signal reporter	Recognition element	Linear range (cfu mL^{-1})	LOD (cfu mL^{-1})	Reference
Fluorescein isothiocyanate	Aptamer	5.64–100	5.07	[30]
Semiconducting polymer dots	Polymyxin B	10^4–10^6	10^4	[31]
Fluorescent organic nanoparticles	Fluorescent organic nanoparticles	4.0×10^3–1.8×10^4	46	[32]
Pyrimidine-based fluorescent probe	Monoclonal antibody	8–301	1.5	[33]
Carbon dots/graphene oxide	Aptamer	10^1–10^7	9	[34]
5-Carboxyfluorescein-labeled complementary DNA/graphene oxide quantum dots	Aptamer	1.28×10^3–2.00×10^7	100	[35]
PDA-PEI copolymer dots	Dual aptamers	10^1–10^7	1	This study

3.4. Specificity and repeatability of the method

The specificity of the method was evaluated by detecting other common foodborne pathogens. The negative control strains (*E. coli* O157:H7, *L. monocytogenes*, *S. aureus*, *S. enterica*) and the target strain (*P. aeruginosa*) were incubated with aptamers@PDA-PEI dots under the same conditions. As shown in Fig. 9, an obvious difference in the fluorescence signal is observed in the presence of *P. aeruginosa*. The difference ($F_0 - F$) in fluorescence signal for the four negative controls are <30% relative to that of *P. aeruginosa*. The excellent specificity of this assay is attributed to the high affinity of the dual-aptamers for target bacteria. Therefore, the method has great potential in selective detection of *P. aeruginosa*.

The parallel samples were respectively measured with the same batch of aptamers@PDA-PEI and different batches of aptamers@PDA-PEI to test the reliability of the method. The intra-assay (same batch) and inter-assay (different batches) relative standard deviations (RSDs, $n = 6$) of this method are all <5.5%, which indicates that the method exhibits good repeatability.

3.5. Real samples analysis

Skim milk, orange juice and popsicle samples were used to validate the feasibility of the method. No bacteria were detected in the blank skim milk, orange juice and melted popsicle samples using the colony counting method. Thus, in order to verify the feasibility of the method in the detection of *P. aeruginosa* in real samples, the spiked skim milk, orange juice and melted popsicle samples with different concentrations of *P. aeruginosa* were used as the test samples.

Since the matrix of real samples are very complex, in order to investigate whether the sample matrix interfere with the detection, the fluorescence intensities of supernatant after centrifugation of aptamers@PDA-PEI in Tris-HCl (20 mM, pH 7.4) and diluted samples were compared. Take the diluted milk sample as an example. As shown in Fig. S6, an obvious decrease (32%) of fluorescence intensity of supernatant is observed for the diluted milk, which demonstrates that the matrix of milk influence the fluorescence intensity of supernatant. In order to avoid the interference from the complex matrix of milk, the sterile milk was used as the blank control. As shown in Fig. S7, the decrease of fluorescence intensity has a good linear relationship with the logarithm of *P. aeruginosa* concentration in the range from 10^1 cfu mL^{-1} to 10^7 cfu mL^{-1} ($R^2 = 0.9520$). Similar experiments were also carried out for orange juice and melted popsicle samples.

As shown in Table 1, the average recoveries of the spiked samples range from 91.4% to 108% with a satisfying analytical precision (RSD ≤ 6.5%). The results indicate that the method is credible in the detection of *P. aeruginosa* in real food samples. More importantly, the centrifugation procedure can effectively eliminate the interference of microparticles in cloudy samples.

The method was compared with previously reported fluorescent methods targeting at detection of *P. aeruginosa* [30–35], as shown in Table 2. The method demonstrates absolute superiority in terms of the linear range and LOD over other methods. More importantly, the method is successfully applied for detection of *P. aeruginosa* in food samples (skim milk, orange juice and popsicle) with intricate matrix. The fabrication of the biosensor and detection procedure are facile. The entire detection process including incubation, centrifugation and fluorescence detection can be finished in 1.5 h, which significantly shortens the detection time for bacteria. Therefore, the biosensor can meet the demand for rapid, selective and sensitive detection of bacteria in food samples.

4. Conclusions

A dual aptamers@PDA-PEI copolymer dots-based biosensor was fabricated and applied for rapid and sensitive detection and quantification of *P. aeruginosa*. Compared to the use of single aptamer, the usage of dual aptamers can efficiently improve the detection sensitivity for fluorescence assay of *P. aeruginosa* since dual aptamers can simultaneously bind to different moieties on cell surface. The LOD of *P. aeruginosa* is as low as 1 cfu mL^{-1}. The result suggests that the use of multiple aptamers for cellular target is effective and superior to the use of single aptamer. Thus, the method provides a universal model for detecting diverse cellular targets just by changing the corresponding aptamers. In addition, the developed method does not require any expensive reagents and sophisticated apparatus, as well as tedious analysis steps. Hence, the aptamers@PDA-PEI dots-based biosensor can serve as an alternative and attractive platform for bacteria detection in food products.

Acknowledgements

This work was supported by the National Natural Science Foundation of China (21675056) and the Scientific and Technological Planning Project of Guangzhou City, China (201805010002).

Appendix A. Supplementary data

Supplementary data to this article can be found online at https://doi.org/10.1016/j.saa.2019.117417.

References

[1] P. Arora, A. Sindhu, N. Dilbaghi, A. Chaudhury, Biosensors as innovative tools for the detection of food borne pathogens, Biosens. Bioelectron. 28 (2011) 1–12.
[2] S. Hameed, L. Xie, Y. Ying, Conventional and emerging detection techniques for pathogenic bacteria in food science: a review, Trends Food Sci. Technol. 81 (2018) 61–73.
[3] J. Chen, B. Park, Recent advancements in nanobioassays and nanobiosensors for foodborne pathogenic bacteria detection, J. Food Prot. 79 (2016) 1055–1069.
[4] Z. Zhong, X. Gao, R. Gao, L. Jia, Selective capture and sensitive fluorometric determination of *Pseudomonas aeruginosa* by using aptamer modified

magnetic nanoparticles, Microchim. Acta 185 (2018) 377.
[5] Y. He, Y. Wang, Y. Shi, Z. Fu, Molecular recognition strategy for detection and antimicrobial susceptibility testing of *Staphylococcus aureus* by utilizing teicoplanin and porcine IgG as indicator molecules, Sens. Actuators B Chem. 267 (2018) 51–57.
[6] Y. Che, Y. Xu, R. Wang, L. Chen, Rapid fluorescence detection of pathogenic bacteria using magnetic enrichment technique combined with magnetophoretic chromatography, Anal. Bioanal. Chem. 409 (2017) 4709–4718.
[7] Q. Wan, Q. Huang, M. Liu, D. Xu, H. Huang, X. Zhang, Y. Wei, Aggregation-induced emission active luminescent polymeric nanoparticles: non-covalent fabrication methodologies and biomedical applications, Appl. Mater. Today 9 (2017) 145–160.
[8] X. Zhang, K. Wang, M. Liu, X. Zhang, L. Tao, Y. Chen, Y. Wei, Polymeric AIE-based nanoprobes for biomedical applications: recent advances and perspectives, Nanoscale 7 (2015) 11486–11508.
[9] Z. Long, L. Mao, M. Liu, Q. Wan, Y. Wan, X. Zhang, Y. Wei, Marrying multicomponent reactions and aggregation-induced emission (AIE): new directions for fluorescent nanoprobes, Polym. Chem. 8 (2017) 5644–5654.
[10] Y. Liu, C. Zhao, K. Fu, X. Song, K. Xu, J. Wang, J. Li, Selective turn-on fluorescence detection of *Vibrio parahaemolyticus* in food based on charge-transfer between CdSe/ZnS quantum dots and gold nanoparticles, Food Control 80 (2017) 380–387.
[11] S. Ahmadian-Fard-Fini, M. Salavati-Niasari, D. Ghanbari, Hydrothermal green synthesis of magnetic Fe_3O_4-carbon dots by lemon and grape fruit extracts and as a photoluminescence sensor for detecting of *E. coli* bacteria, Spectrochim. Acta A Mol. Biomol. Spectrosc. 203 (2018) 481–493.
[12] X. Yang, L. Feng, X. Qin, Preparation of the cf-GQDs-*Escherichia coli* O157:H7 bioprobe and its application in optical imaging and sensing of *Escherichia coli* O157:H7, Food Anal. Methods 11 (2018) 2280–2286.
[13] N. Duan, S. Wu, C. Zhu, X. Ma, Z. Wang, Y. Yu, Y. Jiang, Dual-color upconversion fluorescence and aptamer-functionalized magnetic nanoparticles-based bioassay for the simultaneous detection of *Salmonella typhimurium* and *Staphylococcus aureus*, Anal. Chim. Acta 723 (2012) 1–6.
[14] N. Bhardwaj, S.K. Bhardwaj, J. Mehta, M.K. Nayak, A. Deep, Bacteriophage conjugated IRMOF-3 as a novel opto-sensor for *S. arlettae*, New J. Chem. 40 (2016) 8068–8073.
[15] X. Zhang, S. Wang, L. Xu, L. Feng, Y. Ji, L. Tao, S. Li, Y. Wei, Biocompatible polydopamine fluorescent organic nanoparticles: Facile preparation and cell imaging, Nanoscale 4 (2012) 5581–5584.
[16] M. Liu, J. Ji, X. Zhang, X. Zhang, B. Yang, F. Deng, Z. Li, K. Wang, Y. Yang, Y. Wei, Self-polymerization of dopamine and polyethyleneimine: novel fluorescent organic nanoprobes for biological imaging applications, J. Mater. Chem. B 3 (2015) 3476–3482.
[17] Y. Shi, R. Jiang, M. Liu, L. Fu, G. Zeng, Q. Wan, L. Mao, F. Deng, X. Zhang, Y. Wei, Facile synthesis of polymeric fluorescent organic nanoparticles based on the self-polymerization of dopamine for biological imaging, Mater. Sci. Eng. C 77 (2017) 972–977.
[18] K.-M. Song, S. Lee, C. Ban, Aptamers and their biological applications, Sensors (2012) 612–631.
[19] M. Majdinasab, A. Hayat, J.L. Marty, Aptamer-based assays and aptasensors for detection of pathogenic bacteria in food samples, TrAC Trends Anal. Chem. 107 (2018) 60–77.
[20] K. Wang, Y. Zeng, X. Yang, W. Li, Utility of aptamer-fluorescence in situ hybridization for rapid detection of *Pseudomonas aeruginosa*, Eur. J. Clin. Microbiol. Infect. Dis. (2011) 273–278.
[21] J. Soundy, D. Day, Selection of DNA aptamers specific for live *Pseudomonas aeruginosa*, PLoS One (2017) 1–11.
[22] Z. Zhong, L. Jia, Room temperature preparation of water-soluble polydopamine-polyethyleneimine copolymer dots for selective detection of copper ions, Talanta 197 (2019) 584–591.
[23] C. Zhao, F. Zuo, Z. Liao, Z. Qin, S. Du, Z. Zhao, Mussel-inspired one-pot synthesis of a fluorescent and water-soluble polydopamine-polyethyleneimine copolymer, Macromol. Rapid Commun. 36 (2015) 909–915.
[24] V. Ball, J. Gracio, M. Vila, M.K. Singh, M.-H. Metz-Boutigue, M. Michel, J. Bour, V. Toniazzo, D. Ruch, M.J. Buehler, Comparison of synthetic dopamine–eumelanin formed in the presence of oxygen and Cu^{2+} cations as oxidants, Langmuir 29 (2013) 12754–12761.
[25] H. Xu, X. Liu, D. Wang, Interfacial basicity-guided formation of polydopamine hollow capsules in pristine O/W emulsions - toward understanding of emulsion template roles, Chem. Mater. 23 (2011) 5105–5110.
[26] K. Yamada, T. Chen, G. Kumar, O. Vesnovsky, L.D. Timmie Topoleski, G.F. Payne, Chitosan based water-resistant adhesive. Analogy to mussel glue, Biomacromolecules 1 (2000) 252–258.
[27] Z. Long, M. Liu, R. Jiang, Q. Wan, L. Mao, Y. Wan, F. Deng, X. Zhang, Y. Wei, Preparation of water soluble and biocompatible AIE-active fluorescent organic nanoparticles via multicomponent reaction and their biological imaging capability, Chem. Eng. J. 308 (2017) 527–534.
[28] Z. Long, M. Liu, K. Wang, F. Deng, D. Xu, L. Liu, Y. Wan, X. Zhang, Y. Wei, Facile synthesis of AIE-active amphiphilic polymers: self-assembly and biological imaging applications, Mater. Sci. Eng. C 66 (2016) 215–220.
[29] H. Huang, M. Liu, Q. Wan, R. Jiang, D. Xu, Q. Huang, Y. Wen, F. Deng, X. Zhang, Y. Wei, Facile fabrication of luminescent hyaluronic acid with aggregation-induced emission through formation of dynamic bonds and their theranostic applications, Mater. Sci. Eng. C. 91 (2018) 201–207.
[30] L.H. Kim, H.W. Yu, Y.H. Kim, I.S. Kim, A. Jang, Potential of fluorophore labeled aptamers for *Pseudomonas aeruginosa* detection in drinking water, J. Korean Soc. Appl. Biol. Chem. 56 (2013) 165–171.
[31] Y. Wan, L. Zheng, Y. Sun, D. Zhang, Multifunctional semiconducting polymer dots for imaging, detection, and photo-killing of bacteria, J. Mater. Chem. B 2 (2014) 4818–4825.
[32] G. Kaur, T. Raj, N. Kaur, N. Singh, Pyrimidine-based functional fluorescent organic nanoparticle probe for detection of *Pseudomonas aeruginosa*, Org. Biomol. Chem. 13 (2015) 4673–4679.
[33] S. Ellairaja, N. Krithiga, S. Ponmariappan, V.S. Vasantha, Novel pyrimidine tagged silver nanoparticle based fluorescent immunoassay for the detection of *Pseudomonas aeruginosa*, J. Agric. Food Chem. 65 (2017) 1802–1812.
[34] H. Wang, Z. Chi, Y. Cong, Z. Wang, F. Jiang, J. Geng, P. Zhang, P. Ju, Q. Dong, C. Liu, Development of a fluorescence assay for highly sensitive detection of *Pseudomonas aeruginosa* based on an aptamer-carbon dots/graphene oxide system, RSC Adv. 8 (2018) 32454–32460.
[35] R. Gao, Z. Zhong, X. Gao, L. Jia, Graphene oxide quantum dots assisted construction of fluorescent aptasensor for rapid detection of *Pseudomonas aeruginosa* in food samples, J. Agric. Food Chem. 66 (2018) 10898–10905.